Higher Order Collisionless Ballooning Mode in Tokamaks

A. Hirose, L. Zhang, and M. Elia
Plasma Physics Laboratory, Department of Physics and Engineering Physics, University of Saskatchewan, Saskatoon, Saskatchewan, Canada S7N 0W0
(Received 14 February 1994)

Kinetic stability analysis of general electromagnetic modes in tokamaks has revealed the existence of higher order ballooning mode which is not subject to second stabilization. The kinetic ballooning mode in the magnetohydrodynamic (MHD) second stability region is characterized by eigenfunctions in the ballooning space much broader than that of MHD modes. The ion temperature gradient (η_i) provides the dominant destabilization mechanism.

PACS numbers: 52.35.Fp, 52.35.Kt, 52.55.Fa

The ideal MHD (magnetohydrodynamic) ballooning mode in tokamaks has almost exhaustively been investigated as one of the plausible candidates to impose a limit on the plasma pressure gradient that can be confined stably. Following the numerical discovery of low n (the toroidal mode number) ballooning mode [1,2] and the advent of the ballooning transformation for high n ballooning mode [3–5], the existence of the so-called second stability regime at a sufficiently large pressure gradient has been predicted [6–8]. Currently, some efforts are underway to realize tokamak discharges in the second stability region. The ideal MHD ballooning mode is subject to the usual MHD assumptions, including $E_\parallel \simeq 0$ (sufficiently large plasma conductivity), $|\omega| \gg \omega_*, \omega_D$ (the diamagnetic and magnetic drift frequencies, respectively), and long wavelength nature, $(k_\perp \rho)^2 \ll 1$, where ρ is the ion Larmor radius. These assumptions tend to be dubious at marginal stability where the eigenfunction in the ballooning space becomes broad. Both $\omega_D \propto s\theta \sin\theta$ and $k_\perp^2 = k_\theta^2[1 + (s\theta - \alpha \sin\theta)^2]$ rapidly increase with θ (the extended poloidal angle), and for more satisfactory stability analysis of the ballooning mode, a kinetic theoretic approach is required. [The two-fluid approach to the ballooning mode [9] is still subject to the assumption $(k_\perp \rho)^2 \ll 1$, although the constraint on the frequencies has successfully been removed.]

In order to assess kinetic effects on the conventional MHD ballooning mode based on two-potential approximation, the scalar potential ϕ and parallel vector potential $A_\parallel$, we consider a tokamak discharge with circular magnetic surfaces with the Shafranov shift. For simplicity, the compressional Alfvén (magnetosonic) mode and trapped electrons are ignored. Kinetic effects manifest themselves mainly in the ion density perturbation. For a Maxwellian ion velocity distribution in a low β discharge, the ion density perturbation can be evaluated from the gyrokinetic equation,

$$n_i = -\frac{e\phi}{T_i} n_0 + \left\langle \frac{\omega + \hat{\omega}_{*i}(v^2)}{\omega + \hat{\omega}_{Di}(\mathbf{v}) - k_\parallel v_\parallel} J_0^2\left(\frac{k_\perp v_\perp}{\Omega_i}\right)\left(\phi - \frac{v_\parallel}{c} A_\parallel\right)\right\rangle_{\mathbf{v}} \frac{e}{T_i} n_0, \tag{1}$$

where

$$\hat{\omega}_{*i}(v^2) = \frac{cT_i}{eB^2}\left[1 + \eta_i\left(\frac{Mv^2}{2T_i} - \frac{3}{2}\right)\right][\nabla(\ln n_0) \times \mathbf{B}] \cdot \mathbf{k}_\theta, \tag{2}$$

$$\hat{\omega}_{Di}(\mathbf{v}) = \frac{Mc}{eB^3}\left(\frac{1}{2}v_\perp^2 + v_\parallel^2\right)(\nabla B \times \mathbf{B}) \cdot \mathbf{k}_\perp, \tag{3}$$

are, respectively, the energy and velocity dependent diamagnetic and magnetic drift frequencies, J_0 is the Bessel function, and $\langle \cdots \rangle_{\mathbf{v}}$ indicates velocity averaging with a Maxwellian weighting. For modes in the compressible regime, $|\omega + \omega_{Di}| \gg k_\parallel v_{Ti}$ (v_{Ti} the ion thermal velocity), the ion density perturbation becomes electrostatic,

$$n_i \simeq -\frac{e\phi}{T_i} n_0 + \left\langle \frac{\omega + \hat{\omega}_{*i}(v^2)}{\omega + \hat{\omega}_{Di}(\mathbf{v})} J_0^2 \right\rangle_v \frac{e\phi}{T_i} n_0 = [-1 + I_i(\theta)] \frac{e\phi}{T_i} n_0, \tag{4}$$

where for circular magnetic surfaces with the Shafranov shift assumed in this study,

0031-9007/94/72(25)/3993(4)$06.00

$$I_i(\theta) = \left\langle \frac{\omega + \hat{\omega}_{*i}(v^2)}{\omega + \hat{\omega}_{Di}(\mathbf{v},\theta)} J_0^2\left(\frac{k_\perp(\theta) v_\perp}{\Omega_i}\right)\right\rangle_{\mathbf{v}}, \tag{5}$$

with

$$\hat{\omega}_{Di}(\mathbf{v},\theta) = \frac{Mck_\theta}{eBR}\left(\frac{1}{2}v_\perp^2 + v_\parallel^2\right)[\cos\theta + (s\theta - \alpha\sin\theta)\sin\theta], \tag{6}$$

$$k_\perp^2 = k_\theta^2[1 + (s\theta - \alpha\sin\theta)^2], \tag{7}$$

θ is the extended poloidal angle, and α is the ballooning parameter, $\alpha = -q^2R\,d\beta/dr = q^2R\beta(1+\eta)/L_n$, provided $T_i = T_e$, $\eta_i = \eta_e$, as will be assumed. Here, L_n is the density gradient scale length. Guided by the fluid ion density perturbation in the long wavelength limit derived by Jarmén, Andersson, and Weiland [10], we have found that the following ion density perturbation provides a reasonable approximation which at least qualitatively agrees with exact velocity integral:

$$n_i = -\frac{e\phi}{T_i}n_0 + \left\{\frac{(\omega + \frac{7}{3}\omega_{Di})(\omega + \omega_{*i}) - \eta_i\omega_{*i}\omega_{Di}}{(\omega + \frac{5}{3}\omega_{Di})^2 - \frac{10}{9}\omega_{Di}^2}e^{-\lambda}I_0(\lambda) - \frac{\eta_i(\omega + \frac{5}{3}\omega_{Di})\omega_{*i}\lambda}{(\omega + \frac{5}{3}\omega_{Di})^2 - \frac{10}{9}\omega_{Di}^2}e^{-\lambda}(I_0 - I_1)\right\}\frac{e\phi}{T_i}n_0, \tag{8}$$

where

$$\omega_{Di}(\theta) = \frac{2L_n}{R}\omega_{*i}[\cos\theta + (s\theta - \alpha\sin\theta)\sin\theta], \qquad \lambda(\theta) = \frac{T_i}{M}\frac{k_\theta^2}{\Omega_i^2}[1 + (s\theta - \alpha\sin\theta)^2], \tag{9}$$

and $I_{0,1}[\lambda(\theta)]$ are the modified Bessel functions. Equation (8) may be used for analytic formulation of kinetic ballooning mode. However, in the present numerical investigation, the exact velocity integral in Eq. (4) is employed.

The electron density perturbation in the adiabatic limit $|\omega| \ll k_\parallel v_{Te}$ is

$$n_i = \left(\phi - \frac{\omega - \omega_{*e}}{ck_\parallel}A_\parallel\right)\frac{e}{T_e}n_0. \tag{10}$$

In the regime under consideration ($|\omega + \omega_{Di}| \gg k_\parallel v_{Ti}$), the parallel current is largely carried by electrons,

$$J_{\parallel e} = \frac{n_0e^2}{k_\parallel T_e}\left[(\omega_{*e} - \omega)\phi + \frac{(\omega - \omega_{*e})(\omega - \omega_{De}) + \eta_e\omega_{*e}\omega_{De}}{ck_\parallel}A_\parallel\right]. \tag{11}$$

From the charge neutrality $n_i = n_e$, and parallel Ampère's law, $\nabla^2 A_\parallel = -(4\pi/c)J_{\parallel e}$, we readily obtain the following mode equation for ϕ:

$$\frac{d}{d\theta}\left\{[1 + (s\theta - \alpha\sin\theta)^2]\frac{d\phi}{d\theta}\right\} + \frac{\alpha}{4\epsilon_n(1+\eta)}\left\{(\Omega - 1)[\Omega - f(\theta)] + \eta_e f(\theta) - \frac{(\Omega - 1)^2}{2 - I_i(\theta)}\right\}\phi = 0, \tag{12}$$

where $T_i = T_e$ has been assumed (so that $\omega_{*e} = \omega_{*i}$, $\omega_{De} = \omega_{Di}$), $\Omega = \omega/\omega_*$, and

$$f(\theta) = 2\epsilon_n[\cos\theta + (s\theta - \alpha\sin\theta)\sin\theta]. \tag{13}$$

In the limit of $|\omega| \gg \omega_*$, ω_D, and $\lambda \ll 1$, Eq. (12) readily reduces to the ideal MHD ballooning mode equation

$$\frac{d}{d\theta}\left\{[1 + (s\theta - \alpha\sin\theta)^2]\frac{d\phi}{d\theta}\right\} + \alpha[\cos\theta + (s\theta - \alpha\sin\theta)\sin\theta]\phi + \left(\frac{\omega}{\omega_A}\right)^2[1 + (s\theta - \alpha\sin\theta)^2]\phi = 0, \tag{14}$$

where $\omega_A = V_A/qR$ is the Alfvén frequency.

Equation (12) has been solved numerically with a shooting code for even parity modes. The shooting distance $\theta_{\max}$ is typically 40, but has been varied to ensure that the eigenvalue Ω is independent of $\theta_{\max}$. Figure 1(a) shows the growth rate and mode frequency both normalized by the Alfvén frequency when $L_n/R = 0.175$, $(k_\theta\rho)^2 = 0.01$, $s = 0.4$, $q = 1.2$, $\eta_e = \eta_i = 2$. (These parameters are the same as in Fig. 4 of Ref. [9], obtained from two-fluid approximation to facilitate comparison.) For comparison, the growth rate of the MHD ballooning mode found from Eq. (14) is also shown. In addition to

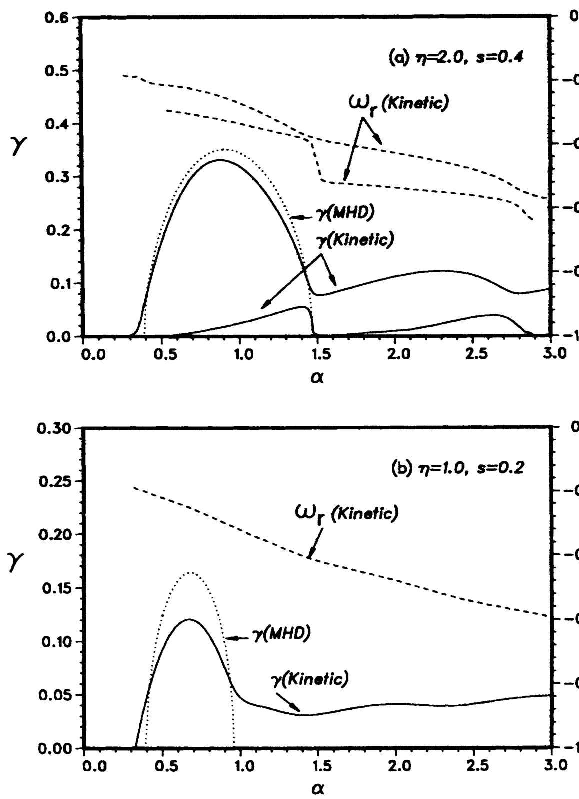

FIG. 1. The growth rate γ and frequency ω_r both normalized by the Alfvén frequency $\omega_A = V_A/qR$ vs. the ballooning parameter α. $q = 1.2$, $(k_\theta \rho)^2 = 0.01$, $\eta_i = \eta_e = 2.0$, $L_n/R = 0.175$, $T_e = T_e$. (a) $s = 0.4$, $\eta_e = \eta_i = 2$, (b) $s = 0.2$, $\eta_e = \eta_i = 1$. For comparison, the growth rate of the ideal MHD mode is depicted by the dotted line.

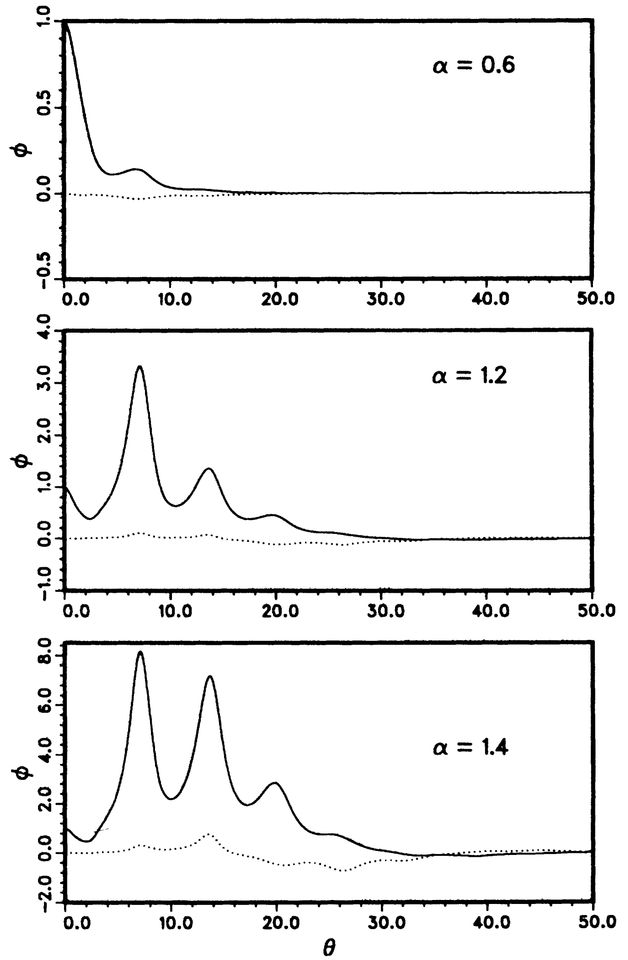

FIG. 2. Eigenfunctions of the kinetic ballooning mode with the same parameters as in Fig. 1(b). From top, $\alpha = 0.6$, 1.2, 1.4. Solid (dotted) lines indicate the real (imaginary) part of $\phi(\theta) = \phi_r + i\phi_i$.

the MHD-like mode labeled 1, there coexists a second mode (2) which persists in the MHD second stability region with growth rate comparable to the MHD mode.

The case at a smaller shear parameter, $s = 0.2$, and less steeper temperature gradients, $\eta = \eta_e = \eta_i = 1.0$, is shown in Fig. 1(b). In this case, the second mode disappears. However, the kinetic ballooning mode persist well above the MHD second stability limit.

The kinetic ballooning modes in the MHD second stability region are characterized by broad eigenfunctions in the θ space. Figure 2 shows eigenfunctions at three values of α for the mode in Fig. 1(b). The case $\alpha = 0.6$ (top) is essentially the MHD mode. The eigenfunction is well confined in the region $|\theta| < 10$, and at small θ, ϕ can be approximated by $\phi = 1 + \cos\theta$. At $\alpha = 1.2$ and 1.4, the MHD mode is stable, but the kinetic mode persists. The eigenfunctions in these cases extend to $\theta \simeq 30$. The effective parallel wave number $k_\parallel$ may be estimated in the following manner:

$$\langle k_\parallel^2 \rangle = -\frac{1}{(qR)^2} \int \phi \frac{d^2\phi^*}{d\theta^2} d\theta \Big/ \int |\phi|^2 d\theta \simeq \frac{0.215}{(qR)^2},$$

which is somewhat smaller than $k_\parallel = 1/\sqrt{3}\,qR$ based on the approximate MHD eigenfunction $\phi = 1 + \cos\theta$, $|\theta| < \pi$.

The stability boundary in the (s, α) plane obtained from the kinetic analysis is summarized in Fig. 3 for the case $\eta = 2$. The MHD stability boundary is also shown for comparison. In the region $s < 0.3$, the first instability boundary is significantly lowered compared with the MHD limit. The second stability region of the MHD ballooning mode practically disappears because of the persistence of the kinetic mode.

The existence of a second ballooning mode has earlier been noted by Cheng [11]. However, its persistence in the second stability regime has not, and constitutes the major finding in the present work. In a comprehensive analysis based on integro-differential equations, Rewoldt, Tang, and Hastie [12] and Tang *et al.* [13] have essentially recovered the MHD ballooning mode. However, the

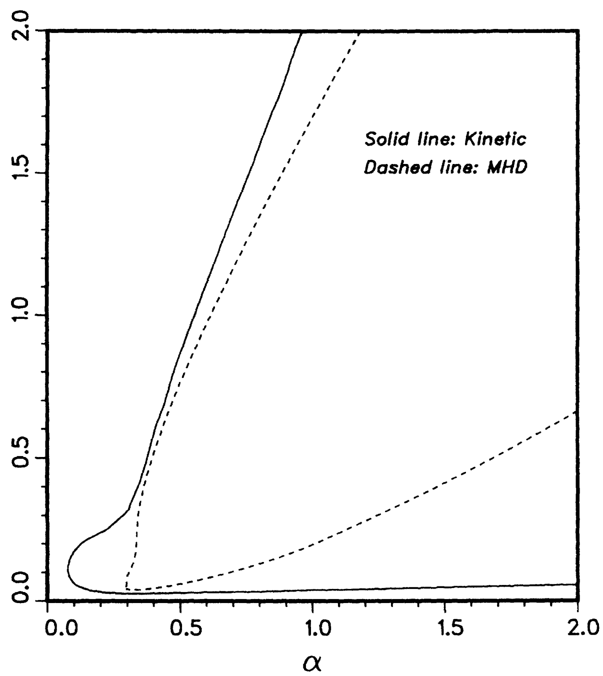

FIG. 3. Stability diagram in the (s, α) plane when $\eta_e = \eta_i = 2$. The dashed line shows the stability diagram of the ideal MHD mode.

second ballooning mode with a broad eigenfunction has not been found. The reason may probably be in truncation of the ballooning variable θ at too small a value. (In Ref. [13], the eigenfunctions of the modes discussed in Ref. [12] are presented. They are confined in the region $|\theta| \lesssim 2\pi$, and can be well approximated by the MHD mode, $\phi = 1 + \cos\theta$.) As shown in Fig. 2, the eigenfunction of the second mode is much broader and extends to $\theta \simeq 30$. In our differential formulation, the kinetic ballooning mode can be revealed only when the shooting distance is chosen at a sufficiently large value.

In this study, trapped electrons, magnetosonic perturbations, and ion transit frequency are all ignored for the purpose to reveal ion kinetic effects on the conventional ideal MHD ballooning mode. The trapped electrons may induce corrections of order $\sqrt{\epsilon}$ where $\epsilon = r/R$ is the inverse aspect ratio. Since the second stability is of practical interest at small shear s which pertains to the core region, ignoring the trapped electron is justifiable in light of the large growth rate of the kinetic ballooning mode found in the second stability region. Effects induced by the magnetosonic mode is at most of order β which is also a small correction. For example, the second stability threshold $\alpha = 0.6$ at $s = 0.1$ corresponds to β_i (the ion beta) = 1.5% for the parameters in Fig. 1(a). The ion transit frequency $k_\parallel v_{Ti}$ also remains small compared with the Doppler shifted frequency $|\omega + \omega_{Di}(\theta)|$ particularly for the kinetic ballooning mode characterized by a broad eigenfunction. [Note that the magnetic drift frequency is oscillatory secular at large θ, $\omega_{Di}(\theta) \propto s\theta\sin\theta$.] We thus believe that all of the effects ignored in the present investigation should not qualitatively modify the growth rate.

In conclusion, a kinetic collisionless ballooning mode of a second kind has been found in the second stability regime. It is characterized by broad eigenfunctions in the ballooning space, and destabilized largely by the ion temperature gradient. Also, the first stability boundary revealed from the kinetic analysis is significantly smaller than predicted from the ideal MHD analysis particularly at small magnetic shear.

Useful comments provided by A. I. Smolyakov and helpful communications with J. Weiland are acknowledged with gratitude. This research has been sponsored by the Natural Sciences and Engineering Research Council, and by the Office of National Fusion Program, Canada.

[1] A. M. M. Todd, M. S. Chance, J. M. Greene, R. C. Grimm, J. L. Johnson, and J. Manickam, Phys. Rev. Lett. **38**, 826 (1977).

[2] D. Dobrott, D. B. Nelson, J. L. Greene, A. H. Glasser, M. S. Chance, and E. A. Frieman, Phys. Rev. Lett. **39**, 943 (1977).

[3] Y. C. Lee and J. W. van Dam, in *Proceedings of the Finite Beta Theory Workshop*, edited by B. Coppi and W. Sadowski (U.S. Department of Energy, Washington, DC, 1977), p. 93.

[4] D. Lortz and J. Nührenberg, Phys. Lett. **68A**, 49 (1977).

[5] J. W. Connor, R. J. Hastie, and J. B. Taylor, Phys. Rev. Lett. **40**, 396 (1978).

[6] C. Mercier, in *Plasma Physics and Controlled Nuclear Fusion Research 1978* (IAEA, Vienna, 1979), Vol. 1, p. 701.

[7] A. Sykes and M. F. Turner, in *Plasma Physics and Controlled Nuclear Fusion Research 1978* (Ref. [6]), p. 625.

[8] L. E. Zhakharov, in *Plasma Physics and Controlled Nuclear Fusion Research 1978* (Ref. [6]), p. 689.

[9] H. Nordman, B. Jhowry, and J. Weiland, Phys. Fluids B **5**, 3465 (1993).

[10] A. Jarmén, P. Andersson, and J. Weiland, Nucl. Fusion **25**, 941 (1987).

[11] C. Z. Cheng, Phys. Fluids **25**, 1020 (1982).

[12] G. Rewoldt, W. M. Tang, and R. J. Hastie, Phys. Fluids **30**, 807 (1987).

[13] W. M. Tang, G. Rewoldt, C. Z. Chang, and M. S. Chance, Nucl. Fusion **25**, 151 (1985).